J. Nano- Electron. Phys.
3 (2011) No1, P. 584-589

PACS numbers: 81.07.De, 85.35.Kt, 71.15.Mb, 81.40.Lm, 62.20.F – , 64.70.K

EFFECT OF RADIAL AND AXIAL DEFORMATION ON ELECTRON TRANSPORT PROPERTIES IN A SEMICONDUCTING SI-C NANOTUBE

S. Choudhary*, ***S. Qureshi***#

IIT Kanpur,
Department of Electrical Engg., Kanpur, India
E-mails: *suds@iitk.ac.in, #qureshi@iitk.ac.in

We study the bias voltage dependent current characteristic in a deformed (8, 0) *silicon carbide nanotube by applying self consistent non-equilibrium Green's function formalism in combination with the density-functional theory to a two probe molecular junction constructed from deformed nanotube. The transmission spectra and electron density of states at zero bias shows a significant reduction in threshold in the case of both radially compressed and axially elongated nanotube. However, semiconductor to metal transition was not observed, though the results show large differences in current characteristic compared to a perfect nanotube.*

Keywords: *NANOTUBE, SiCNT, ARMCHAIR-ZIGZAG, DEFECTS, DEFORMATION.*

(Received 04 February 2011, in final form 15 June 2011)

1. INTRODUCTION

The high energy difference between the sp2 and sp3 bonds (1.25 eV per Si-C pair) [1], which makes the existence of a silicon carbide (SiC) graphitic phase impossible, has not obstructed the scientists from synthesizing SiC nanotubes (SiCNTs) [2, 3]. Recently, the scientists have suggested to make silicon carbide nanotubes (SiCNTs) as a possible alternative to carbon nanotubes (CNTs) for field emitting applications [2, 3], which has boosted the interest for SiCNTs and several studies on the electronic properties of SiCNTs can be found in the literature [4-8]. It is well known that CNTs undergo a semiconductor to metal transition (SMT) [4] or metal to semiconductor transition (MST) [5] when deformed. Therefore, it is of interest to understand how the electronic properties of SiCNTs would get altered when deformed.

It is known that SiCNTs are generally semiconductors, except for the (3, 0) and (4, 0) nanotubes which are metals [6], and the band gap (E_g) is wider for larger tube diameters [3, 7]. However, another study [8] suggests that in the range $n = 7 - 10$, (n, n) nanotubes are semiconductors and their band gap decreases steadily with increasing n, nanotubes with $n = 5$ and 6 are metallic. Also, at $n = 7 - 9$, (n, 0) nanotubes are semiconductors, and their band gap increases steadily with n, nanotubes with $n = 5$ and 6 have metallic conductivity. An applied uniaxial strain results in the modification of both E_g width and band structure of SiCNTs [9] which was also observed for CNTs [4], the effects of radial compression along with axial elongation on the electronic properties of SiCNTS have not been studied so far.

In the present work, we investigate the electronic properties by studying the transmission energy spectrum $T(E)$, density of states (DOS) and current-voltage (I-V) characteristics of a (8, 0) SiCNT under both radial compression and axial elongation. The electron transport calculations were carried out on an ab initio based simulator called Atomistix [10] which uses density functional theory (DFT) and non equilibrium Green's functions formulations (NEGF) together for obtaining electronic transport properties of molecules and devices. More details about the method and software could be found in previous reports [11-13].

2. SIMULATION SETUP

A perfect (non-deformed) SiCNT is shown in Fig. 1 a with Si-C bond length of 1.78 A [3, 9] and 1:1 Si-C ratio, whereas in Fig. 1 b, a radially deformed nanotube compressed in XY-coordinates (XY-distortion) is shown. The degree of radial compression or XY-distortion is determined by the XY ratio of the ellipse. When the tube is stretched in Z-coordinate (Z-distortion), an axially elongated or axially deformed nanotube results. The stretch factor in Z-coordinate determines the amount of elongation deformation. We used Nanotube Modeler [14] for creating above kind of deformed SiCNT structures, which generates XYZ-coordinates of nanotubes. The above structures were exported to Atomistix [10] for setting up a two probe geometry which consists of a left electrode, right electrode and a central region (Fig. 1 c).

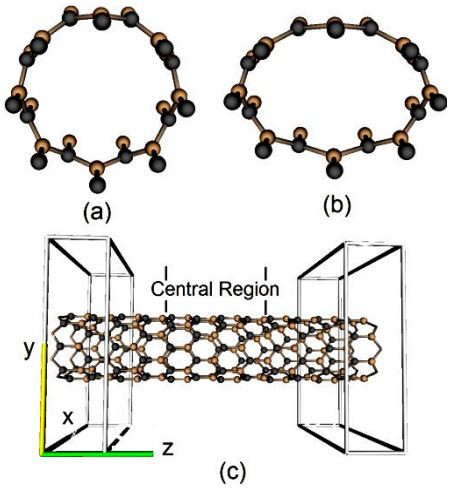

Fig. 1 – (8, 0) SiCNT (*a*) *Non deformed,* (*b*) *Radially deformed and* (*c*) *two probe system of deformed* (8, 0) SiCNT *with a central region and left-right electrodes*

The electron transport characteristic of a SiCNT may depend on its length, resistance, contacts and applied bias. We neglect length dependency by considering a minimal length segment of nanotube in the central region. In order to minimize the contact dependency, SiCNT electrodes with deformation similar to the central region are used to construct the two probe system of Fig. 1 c. The lengths of the central regions, screening layers and the electrodes of the simulated sections are taken as 8 periods (32 C

atoms and 32 Si atoms), 2 periods (16 C atoms and 16 Si atoms) and 2 periods (16 C atoms and 16 Si atoms), respectively. Hence, a central region width of 9.79 Å (SiCNT length) for non deformed and radially deformed case, 10.28 A for Z 1.05 and 10.77 Å for Z 1.1 axial elongation cases, are used in the simulation.

The simulation parameters were selected to provide accurate measurements as reported for CNTs [15] and are following: mesh cut-off energy was 400 Ry, basis set was double zeta polarized with 0.001 Bohr radial sampling, exchange correlation functional was set to local density approximation (LDA) type with double zeta polarized (DZP) basis set, Brillouin zone integration parameters of electrodes are taken as (1, 1, 500). Electrode temperature was set to 1000 K which makes the convergence easier; it has no effect on the overall measurement which was also verified at lower electrode temperatures. Due to the requirement of heavy computing resources, we used the above parameters, which shall ensure convergence without any necessity of repeating simulations.

3. SIMULATION RESULTS AND ANALYSIS

Simulation results are presented in Fig. 2, where I-V characteristic is shown and in Fig. 3, where zero bias transmission energy spectrum $T(E)$ and density of states DOS results are shown. Let us first look at the bias voltage dependent current with modulated deformation. Note that since we are using semiconducting (8, 0) SiCNT electrodes, initially there will be no current in the system. But in the case of deformed SiCNTs with deformed electrodes there will be current because the deformation changes the conducting properties of (8, 0) SiCNT in the central region as well as (8, 0) SiCNT electrodes. Our assumption of semiconducting electrodes (to minimize the contact dependency) will certainly not match experimental values of the current obtained using metallic electrodes, but is fair enough to comment on the changes in the conducting properties of the SiCNT under applied deformation. An axial elongation with a stretch factor of Z 1.05 (Z-distortion) results in a small increment in current compared to non deformed case. Nanotube was further stretched to Z 1.1 to see any change in current, a small increment was observed. Next, we radially deformed the SiCNT with XY-distortion of XY 1.3 and observed orders of magnitude of increment in current. A small increment in current was further observed when both radial and axial deformations (XY 1.3 Z 1.05) were applied simultaneously. The radial deformation was further increased to XY 1.5 while axial elongation fixed at Z 1.05, large increment in current was observed for both low and high bias voltages which suggest a reduced threshold in SiCNTs. However, semiconductor to metal transition (SMT) was not observed here, whereas, a SMT was demonstrated in the case of CNTs in literature [4]. The SiCNTs could have been deformed further to observe any possibility of SMT but further deformation results in breaking of Si-C bonds.

To gain more insight of I-V characteristic, we study T (E) and DOS results of the ideal and deformed SiCNTs, and compare them. The electrode interaction in two probe method results in bandgap variations. Hence, it is not useful to compare the I-V curve obtained using two probe method with the aid of band diagram. Transmission spectrum is the best way to explain I-V curve of these systems which has also been used by [15] to explain I-V curve. The transmission

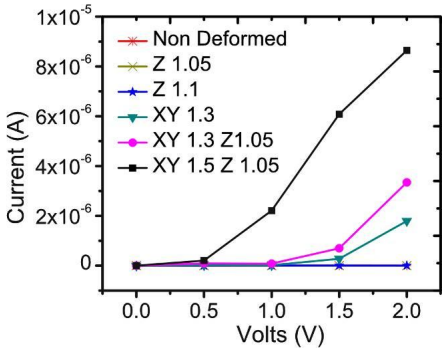

Fig. 2 – *Bias voltage dependent current characteristic* (I-V *characteristic*) *of* (8, 0) SiCNT *two probe system. Current is shown to vary with modulation in radial and axial deformation*

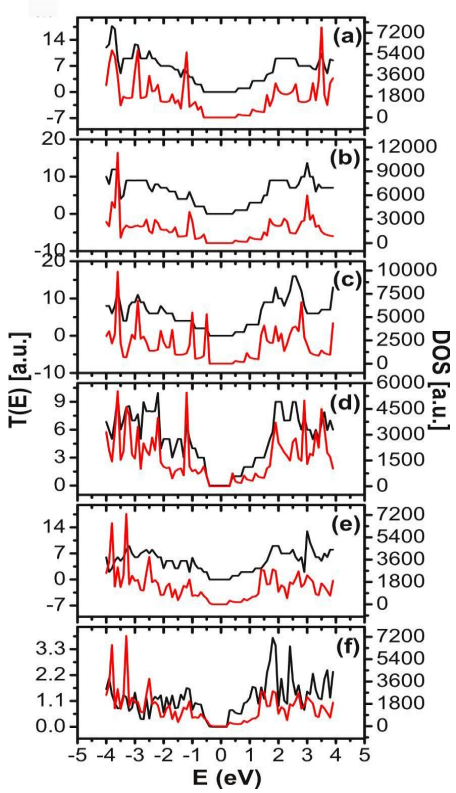

Fig. 3 – *Zero bias transmission spectra* $T(E)$ *and density of states* DOS *profile of* (8, 0) SiCNT (*a*) *Non deformed*, (*b*) - (*c*) *axial stretching deformation with stretch factor* Z 1.05 *and* Z 1.1, *respectively*, (*d*) *radial compression deformation with XY-distortion as* XY 1.3 *and* (*e*) - (*f*) *both radial and axial deformations applied simultaneously as* XY 1.3 Z 1.05 *and* XY 1.5 Z 1.05, *respectively.* DOS *is number of electrons/energy, i.e. unit* 1/*eV*. [***Note:*** *a.u. is arbitrary units and* E *is energy in electron volts*]

spectrum describes the probability for electron with incident energy E to transfer from the left electrode to the right electrode and the integral of the transmission spectrum yields the current through the system [11].

The equation for calculating current from the transmission spectrum can be found in literature [11]. The equilibrium transport properties (no bias voltage applied) of the two-probe model were investigated firstly. The T (E) in Fig. 3 is shown by black curve in which the Fermi energy is set as 0 eV [11], DOS is shown by red curve. The T (E) for non deformed case is shown in Fig. 3 a, which reflects the semiconducting nature of SiCNT with a wide transmission gap seen as a flat curve around Fermi level (0 eV). Fig. 3 b - f presents the T (E) and DOS with modulation in deformation similar to that in I-V characteristic analysis described above. Small reduction in transmission gap around Fermi level was observed with the increase of radial deformation due to bandgap reduction with applied deformation, which results in increase in current. The band gap variation with deformation is attributed to the change of the electron orbital overlap caused by the bond length variation under deformation, which was also stated in [9]. We observed the bandgap variations through molecular projected self-consistent Hamiltonian (MPSH) by finding the difference of HOMO (Highest Occupied Molecular Orbital) and LUMO (Lowest Unoccupied Molecular Orbital) level. The transmission width reduction on varying deformation, at zero bias, could also be seen in Fig. 4 a where the T (E) curves are superimposed.

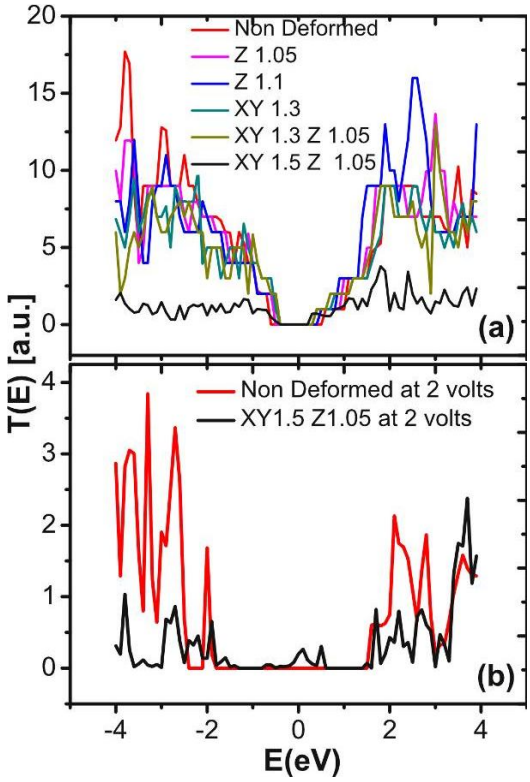

Fig. 4 – (*a*) *Zero bias transmission spectra and* (*b*) *transmission spectra at* 2 *volts*

For further investigation of high current characteristic, we studied the transmission spectra at a bias voltage of 2 volts and compare it with the non deformed case. Transmission spectra for non deformed SiCNT and deformed case with XY 1.5 Z 1.05 distortion are shown in Fig. 4 b. For non deformed case, we see that transmission gap around the Fermi level is nearly flat, but there are peaks in case of deformed SiCNT. These peaks in the transmission gap around Fermi level suggests further reduction in bandgap, resulting in an increase in current which reduces the threshold voltage as observed in the I-V characteristic of Fig. 2.

4. CONCLUSION

In summary, the results show a reduction in threshold voltage in case of radial compression and axial elongation applied simultaneously in (8, 0) semiconducting SiCNT. Transmission gap reduction around Fermi level with applied deformation was observed, which is due to the bandgap reduction that results in increase in current. However, semiconductor to metal transition was not observed in the cases of deformations considered in this study.

REFERENCES

1. Y. Miyamoto, B. D. Yu, *Appl. Phys. Lett.* **80**, 586 (2002).
2. T. Taguchia, N. Igawaa, H. Yamamotoa, S. Shamotoa, S. Jitsukawa, *Physica E* **28**, 431 (2005).
3. G. Alfieri, T. Kimoto, *Appl. Phys. Lett.* **97**, 043108 (2010).
4. Y. Ren, K. Q. Chen, Q. Wan, B. S. Zou, Y. Zhang, *Appl. Phys. Lett.* **94**, 183506 (2009).
5. J.Q. Lu, J. Wu, W. Duan, F. Liu, B.F. Zhu, B.L. Gu, *Phys. Rev. Lett.* **90**, 156601 (2003).
6. I.J. Wu, G.Y. Guo, *Phys. Rev. B* **76**, 035343 (2007.)
7. M. Zhao, Y. Xia, F. Li, R.Q. Zhang, S.T. Lee, *Phys. Rev. B* **71**, 085312 (2005).
8. E.V. Larina, V.I. Chmyrev, V.M. Skorikov, P.N. Dyachkov, D.V. Makaev, *Neorganicheskie Materialy* **44**, 934 (2008).
9. Z. Wang, X. Zu, H. Xiao, F. Gao, W. J. Weber, *Appl. Phys. Lett.* **92**, 183116 (2008).
10. Atomistix, www.quantumwise.com.
11. M. Brandbyge, J. L. Mozos, P. Ordejyn, J. Taylor, K. Stokbro, *Phys. Rev. B* **65**, 165401 (2002).
12. J. Taylor, H. Guo, and J. Wang, *Phys. Rev. B* **63**, 245407 (2001).
13. J.M. Soler, E. Artacho, J.D. Gale, A. Garcia, J. Junquera, P. Ordejyn, D. Sanchez-Portal, *J. Phys.: Condens. Matter* **14**, 2745 (2002).
14. Nanotube Modeller, http://www.jcrystal.com/.
15. S. Yamacli, M. Avci, *Phys. Lett. A* **374**, 297 (2009).